ISSN: 2096-3246
Volume 58, Issue 01, 2026

CONJUGATE HEAT TRANSFER ANALYSIS OF A HEAT EXCHANGER USING VARIOUS COMBINATIONS OF NANOPARTICLES AND BASE FLUIDS

Ritesh Tiwari[1*]; Dr.Chitresh Nayak[2]
[1*]Research Scholar;
Department of Mechanical Engineering, Medicaps University, Indore (Bharat).
Email id: rt1725553@gmail.com
[2] Professor,
Department of Mechanical Engineering, Medicaps University, Indore (Bharat).
Email id :chitresh.nayak@medicaps.ac.in

Abstract
This study experimentally and analytically investigates the thermal performance enhancement of shell-and-tube heat exchangers using nanofluids, with a focus on conjugate heat transfer analysis. Five nanoparticle types (Al_2O_3, ZnO, SiO_2, CuO, and TiO_2) dispersed in distilled water and ethylene glycols were evaluated. The conjugate analysis integrates fluid-thermal-structural interactions, revealing that ethylene glycol-based nanofluids exhibit more stable heat transfer characteristics (19.83% deviation in HTC from theory) compared to water-based systems (93.33% deviation). SiO_2 nanoparticles showed consistent performance across all parameters, while CuO displayed significant variability in ethylene glycol (LMTD deviations up to 14.68%). The study highlights limitations in theoretical models, particularly at higher nanoparticle concentrations (4–5%), where particle aggregation and interfacial thermal resistance dominate. Conjugate modeling demonstrated that water-based nanofluids achieve 10X higher heat flux than ethylene glycol due to superior conductivity, though EG's lower viscosity reduces pumping costs.
Keywords: Nanofluids, base fluids, heat exchanger, conjugate heat transfer.

1. INTRODUCTION

Nano fluids have been shown to possess enhanced thermo physical properties such as higher thermal conductivity, improve thermal diffusivity, modified viscosity and enhanced convective heat transfer coefficients when compared to traditional coolants (Ali and Salam, 2020).

The use of nanofluids as heat transfer media enables more compact system designs, allowing smaller radiators to replace larger ones and offering greater flexibility in their placement in automotive and other thermal management applications. One of the most effective strategies for improving the heat transfer performance of conventional fluids is the suspension of ultrafine solid particles within them (Sharif et al., 2016). These particles may be metallic (e.g., Cu, Ag) or non-metallic (e.g., CuO, Fe_2O_3, Al_2O_3, TiO_2), and their incorporation into the base fluid significantly alters the fluid's thermal behavior. By leveraging the enhanced thermal characteristics imparted by nanoparticles, nanofluids have emerged as a promising alternative for overcoming the inherent limitations of traditional heat transfer fluids.

Industrial process, according to Nivedini et al. (2020), relies significantly on thermal energy for heating and cooling processes. Industrial processes demand high heat transfer performance for efficiency and low energy loss (Karuppasamy et al., 2019). Reducing energy wastage demands techniques that can provide high heat transfer

rates at the same time minimizing losses to the bare minimum. Traditional extended surface techniques, such as fins and microchannels, commonly used in vehicles and electronic devices, are now getting close to their performance limits. Advanced methods thus revolve around optimized surface geometries or the introduction of fluid-based additives for improved thermal performance (Said *et al.,* 2019). Compound heat transfer techniques, involving the use of two or more enhancement methods in combination, offer further scope. However, common coolants such as water, engine oil, and ethylene glycol employed in most heat exchangers have comparatively low thermal conductivity, which curtails their performance. New technologies capable of significantly improving the thermal properties of the cooling fluid have thus become a subject of widespread research interest.

The application of nanofluids in heat exchangers has been a topic of interest over the last decade, a testament to their significant potential for increasing the efficiency of thermal systems. Nanofluids are defined by the suspension of solid nanoparticles in a base heat transfer fluid, and this is associated with enhanced thermal properties, such as enhanced thermal conductivity and enhanced heat transfer coefficients (Hussein & Issa, 2023; Salim et al., 2024; Porgar et al., 2023). All these properties position them as among the leading candidates for the use as a substitute for conventional coolants in industrial applications. Vallejo et al. (2022) affirm that the number of studies targeting nanofluids has grown exponentially in the last two decades, and initial studies were mainly concentrating on mono nanofluids, a single nanoparticle suspended in a base fluid. Notwithstanding the continued challenges, among them dispersion stability issues and increased pumping power requirements, nanofluids have been extremely successful as working fluids, especially in energy and thermal management systems where they can enable notable improvements in the efficiency of heat exchangers.

Al_2O_3 and CuO metal oxide nanoparticles-dispersed nanofluids have exhibited adequate promise for heat transfer efficiency enhancement in a broad variety of heat exchanger geometries. Shabi et al. (2024) exhibited noteworthy improvement of the Al_2O_3 nanofluid heat transfer rate in shell-and-tube and helically coiled heat exchangers, especially with optimal geometrical parameters. Likewise, Nallusamy and Babu (2015) showed hybrid aluminum oxide and copper nanoparticles in water suspension to have substantially improved the thermal conductivity, with improved shell-and-tube heat exchanger performance. Iqbal et al. (2021) observed impact of the nanofluid thermophysical properties on energy transfer optimization, with implications in nuclear systems as well. Anggono et al. (2023) also investigated the impact of the flow rate and nanoparticle concentration on carbon nanotube-based nanofluids, with strong correlation of these with increased convective heat transfer coefficients—a critical parameter for optimized advanced heat exchanger design. According to Ismail *et al.* (2025), due to urbanization, industrialization and population growth, global energy consumption continues to rise. Similarly, Kamusuwan *et al.* (2025) also reported that in the current century, due to rapid global population growth, the need of energy and waste removal has increased a lot.According to Nivedini *et al.* (2020), the industrial sector mainly functions on the usage of thermal energy for their heating and cooling systems. Heat transfer magnification is demanded in many industrial applications (Karuppasamy *et al.*, 2019).

Enhancement of heat transfer with high rate and reduction of energy losses is most important for researchers to deal with the energy wastage problems. To achieve this extended surface technologies such as fins, micro channels with common automobiles, electronic machineries are reaching to their limits (Kunti *et al,.* 2020). The advanced techniques require special type

of surface geometries or fluid additives to increase the heat transfer rate. In Compound heat transfer technique we use the combination of any two or three above mentioned techniques simultaneously. Conventional coolants which are used in different type of heat exchanger such as water, engine oil, ethylene glycol etc. have poor or low heat transfer rate. Therefore, new technologies which have potential to improve the thermal properties of cooling fluids are of great interest to the researchers. In this series, Uddin *et al.* (2024) reported that due to their promising potential in enhancement in heat transfer, nanofluids containing tiny nanoparticles (1–100 nm) have attracted researchers.According to Generous *et al*. (2023) these fluids are simply fluids in which very fine nanoparticles are mixed with a base fluid. Because of this special combination, they show different and unique behaviour compared to normal fluids. Their main advantages are higher thermal conductivity, better heat transfer, and in some cases special optical and magnetic properties. Due to these qualities, nanofluids are considered a promising option for improving heat transfer in practical applications.According to Awais *et al*. (2021) Nanofluids, as next-generation heat transfer media, have gained wide research attention due to their high effectiveness. The addition of nanoparticles with superior thermal conductivity enhances heat transfer with only moderate pumping power. Their use in systems like solar thermal units, HVAC, electronics, heat exchangers, and nuclear reactors improves efficiency and also supports efforts to reduce climate change impacts.

Based on careful study it has been found that limited articles were focused on conjugate heat transfer analysis of heat exchanger and few works were found which were focused on applications of different combinations of nanofluids and base fluids. Considering these facts the present research work is devoted to the investigations on thermal performance of heat exchanger with different combinations of nanofludids and basefluids. We focus on the investigations considering thermal properties of different nannofluid-basefluid combinations for a case heat exchanger. *Using* **conjugate analysis** we characterize the significant effects of *thermal properties of nanofluid-basefluid combinations.* Ethylene glycol-based nanofluids show more stable heat transfer characteristics than water-based fluids. SiO_2 nanoparticles exhibits excellent performance over all parameters. The observations show some limitations in theoretical models at higher nanoparticle concentrations. Through Conjugate analysis it is shown that water-based nanofluids exhibits higher heat flux than ethylene glycol.

2. MATERIALS AND METHODS

A. Theoretical basis

Present section focuses on the details of calculations used for investigations of physical and thermal properties of nanofluid-basefluid alternatives, and thermal properties, the details of which are presented in upcoming sub-sections.

Physical Properties of Nanofluid-Basefluid Alternatives

The following are the details of calculations for physical properties of nanofluid–basefluid combinations (Kleinstreuer and Yu Feng, 2011):The density of the nanofluid was determined using the relation suggested by Kleinstreuer and Yu Feng (2011), where ρ_{np}shows the density of nanoparticles, ρ_{bf} is the density of the base fluid, and φ denotes the molar concentration of nanoparticles dispersed in the base fluid. This equation accounts for the contribution of both the base fluid and the nanoparticles to the overall density of the nanofluid

based on their respective proportions in the mixture. Hence,

$$\rho_{nf} = (1 - \varphi) \times \rho_{bf} + \varphi \times \rho_{np,}\text{as} \quad (1)$$

Specific heat of the Nanofluid was calculated using following equation (Puspitasari *et al.*, 2020):

$$C_{p_{nf}} = (1 - \varphi) \times C_{p_{bf}} + \varphi \times C_{p_{np}} \quad (2)$$

.....where,
$C_{p_{nf}}$~ Specific heat of Nanofluid;
$C_{p_{bf}}$~ Specific heat of base fluid;
$C_{p_{np}}$~ Specific heat of nano-particles;
φ~ Molar concentration of nanoparticles in the base fluid.

Thermal conductivity of the Nanofluid was calculated using following equation (Puspitasari *et al.*, 2020):

$$\frac{k_{nf}}{k_{bf}} = 1 + \frac{3(\frac{k_{np}}{k_{bf}} - 1) \times \varphi}{(\frac{k_{np}}{k_{bf}} + 2) - (\frac{k_{np}}{k_{bf}} - 1) \times \varphi} \quad (3)$$

.....where,
k_{np}~ Density of nanoparticles
k_{bf}~ Density of base fluid
φ~ Molar concentration of nanoparticles in the base fluid.

Viscosity the Nanofluid was calculated using following equation (Colla*et al.*, 2012):

$$\mu_{nf} = \mu_{bf} \times (1 + 2.5 \times \varphi + 6.5 \times \varphi^2) \quad (4)$$

.....where,
μ_{nf}~Viscosity of nanofluid
μ_{bf}~ Viscosity of base fluid
φ~ Molar concentration of nanoparticles in the base fluid.

Thermal Properties of Nanofluid-Basefluid Alternatives

The following parameters were used for the calculation of thermal properties of nanofluid–basefluid combinations (Incropera *et al.*, 2017). The **heat transfer coefficient (h)** measures how effectively heat is transferred between a solid surface and a fluid (or between two fluids). It quantifies the thermal conductance per unit area (W/m²·K).

$$h = \frac{q}{\Delta T} \quad (5)$$

…..where,
h ~ heat transfer coefficient (W/m²·K)
q ~ heat flux (W/m²)
ΔT ~ temperature difference between surface and fluid (K)

The Log Mean Temperature Difference (LMTD) shows the average temperature driving

force for heat transfer in a heat exchanger, accounting for varying temperature differences between hot and cold fluids.

$$LMTD = \frac{\Delta T_1 - \Delta T_2}{ln\left(\frac{\Delta T_1}{\Delta T_2}\right)} \quad (6)$$

…..where,
$\Delta T_1 \sim T_{hot,in} - T_{cold,out}$
$\Delta T_2 \sim T_{hot,out} - T_{cold,in}$

The heat transfer rate is the total amount of thermal energy transferred per unit time (W or J/s) in a system, often calculated using the overall heat transfer coefficient and LMTD.

$$Q = U.A.\ (LMTD) \quad (7)$$

…..where,
Q ~ heat transfer rate (W)
U ~ overall heat transfer coefficient (W/m²·K)
A ~ heat transfer area (m²)

Analytical Conjugate Heat Transfer Model

The following parameters were used in this work (Increopera *et al.,* 2017)
The thermal interaction between nanofluids and heat exchanger walls is modeled using lumped thermal resistance networks and one dimensional heat conduction.

$$Q = \frac{\Delta T_{overall}}{R_{total}}, R_{total} = R_{conv,h} + R_{cond} + R_{conv,c} \quad (8)$$

…..where,
$R_{conv,h}$~ convection in hot nanofluid
R_{cond}~ Conduction through tube walls
$R_{conv,c}$ ~ convection in cold nanofluid

$$R_{conv} = \frac{1}{h.A} \quad (9)$$

…..where,
$h \sim Experimental\ HTC$

For cylindrical tubes walls, the conductive resistance is represented as follows:

$$R_{cond} = \frac{In\left(\frac{r_o}{r_i}\right)}{2\pi L k_{wall}}, k_{wall} = 401 \quad (10)$$

At steady state, heat flux matches at the fluid-wall interface:

$$T_{wall} = T_{fluid} + \frac{Q}{h.A} \quad (11)$$

The properties of nano particles and base fluids were investigated form the previous works, as follows.

Table 1: Properties of Base Fluids, Nanofluids and Heat Exchanger Materials

(Kleinstreuer Feng, 2013;Puspitasari *et al.*, 2020; Colla *et al.*, 2012)

S. No	Material	Density (kg m-3)	Specific Heat (J kg-1 K-1)	Thermal Conductivity (W m K-1)
1.	Water	996	4178	0.615
2.	Ethylene Glycol	1110	2360	0.254
3.	Al_2O_3	3970	775	39
4.	TiO_2	4000	711	8.04
5.	CuO	6500	525	17.65
6.	ZnO	5600	540	54
7.	SiO_2	2200	745	1.4
8.	Copper (tubes)	8960	385	385
9.	Mild steel (shell)	7850	500	50

b) In next step, properties of nanofluids-basefluid alternatives and base fluids were calculated, by using equations provided in last section, as shown below.

Table 2: Properties of Nanofluid-Basefluid Alterantives and Base fluids

S.No	Alterative	Percentage composition of nanofluids in basefluids																			
		1% Percent				2% Percent				3% Percent				4% Percent				5% Percent			
		Density	Sp. Heat	Th.	Viscosity	Density	Sp. Heat	Th.	Viscosity	Density	Sp. Heat	Th.	Viscosity	Density	Sp. Heat	Th.	Viscosity	Density	Sp. Heat	Th.	Viscosity
1.	Al_2O_3-Distilled Water	1026.9	4001	0.647	0.00091	1071.6	3734	0.698	0.00094	1101.4	3556	0.732	0.00097	1131.2	3378	0.766	0.00099	1161	3200	0.8	0.00102
2.	Al_2O_3-Ethylene Glycol	1162.9	2371	0.268	0.0161	1235.8	2305	0.292	0.017	1284.4	2261	0.308	0.0176	1333	2217	0.324	0.0181	1381.6	2173	0.34	0.0186
3.	ZnO - Distilled Water	1054.9	3941	0.641	0.00091	1139.6	3584	0.683	0.00094	1195.4	3346	0.711	0.00097	1251.2	3088	0.739	0.00099	1307	2850	0.767	0.00102
4.	ZnO-Ethylene Glycol	1178.9	2341	0.264	0.0161	1275.8	2230	0.282	0.017	1340.4	2156	0.294	0.0176	1405	2085	0.306	0.0181	1469.6	2017	0.318	0.0186
5.	SiO_2-Distilled Water	1008.9	4101	0.617	0.00091	1026.6	3984	0.623	0.00094	1038.4	3906	0.627	0.00097	1050.2	3828	0.631	0.00099	1062	3750	0.635	0.00102

6.	SiO_2-Ethylene Glycol	1136.9	2395	0.254	0.0161	1170.8	2365	0.257	0.017	1193.4	2345	0.259	0.0176	1218	2325	0.261	0.0181	1243.6	2305	0.263	0.0186
7.	CuO-Distilled Water	1060.9	3881	0.651	0.00091	1154.6	3434	0.708	0.00094	1216.4	3136	0.746	0.00097	1278.2	2838	0.784	0.00099	1340	2540	0.822	0.00102
8.	CuO-Ethylene Glycol	1188.9	2325	0.27	0.0161	1300.8	2190	0.297	0.017	1375.4	2100	0.315	0.0176	1453	2010	0.333	0.0181	1529.6	1920	0.351	0.0186
9.	TiO_2-Distilled Water	1032.9	3981	0.627	0.00091	1086.6	3684	0.648	0.00094	1122.4	3486	0.662	0.00097	1158.2	3288	0.676	0.00099	1194	3090	0.69	0.00102
10.	TiO_2-Ethylene Glycol	1164.9	2365	0.26	0.0161	1240.8	2290	0.272	0.017	1291.4	2240	0.28	0.0176	1341	2190	0.288	0.0181	1392.6	2140	0.296	0.0186
11.	Water (pure)	997	4,182	0.61	0.000	Properties and their units: Density in kg/m^3 Sp. Heat in J/kg-K Th. Cond. In W/m-K Viscosity in Pa-s															
12.	Ethylene Glycol (pure)	1,113	2,380	0.26	0.0158																

B. Experimental Approach

The following stepwise procedure was adopted to solve the problem using experimental approach: In the next stage of the study, the physical and thermal properties of the nanofluid were examined analytically and experimentally using a shell and tube heat exchanger (Figure 1(a)) with an inner shell diameter of 230 mm, shell thickness of 6 mm, and a length of 550 mm for both the shell and tubes; the system consisted of five copper tubes having an outer diameter of 16 mm and inner diameter of 13 mm, enclosed within a mild steel (MS) shell. The flow configuration was counter-flow, maintained at a rate of 2 liters per minute, with hot water entering at 80 °C and cold water at 27 °C, enabling effective thermal exchange and accurate assessment of heat transfer characteristics for the nanofluid–base fluid combination. Figure 1(b) shows the picture of various components of experimental setup.

In addition to the shell-and-tube heat exchanger, the experimental arrangement included several supporting components required for controlled circulation and temperature regulation of the working fluids. A hot water generation unit equipped with an electric heating system was used to attain the desired inlet temperature on the tube side, while a separate storage reservoir supplied the cooling water to the shell side. Fluid circulation was maintained through centrifugal pumps connected by flexible hoses, and the flow rate in each stream was regulated by rotameters to maintain a constant discharge of 2 L/min throughout the tests.

ISSN: 2096-3246
Volume 58, Issue 01, 2026

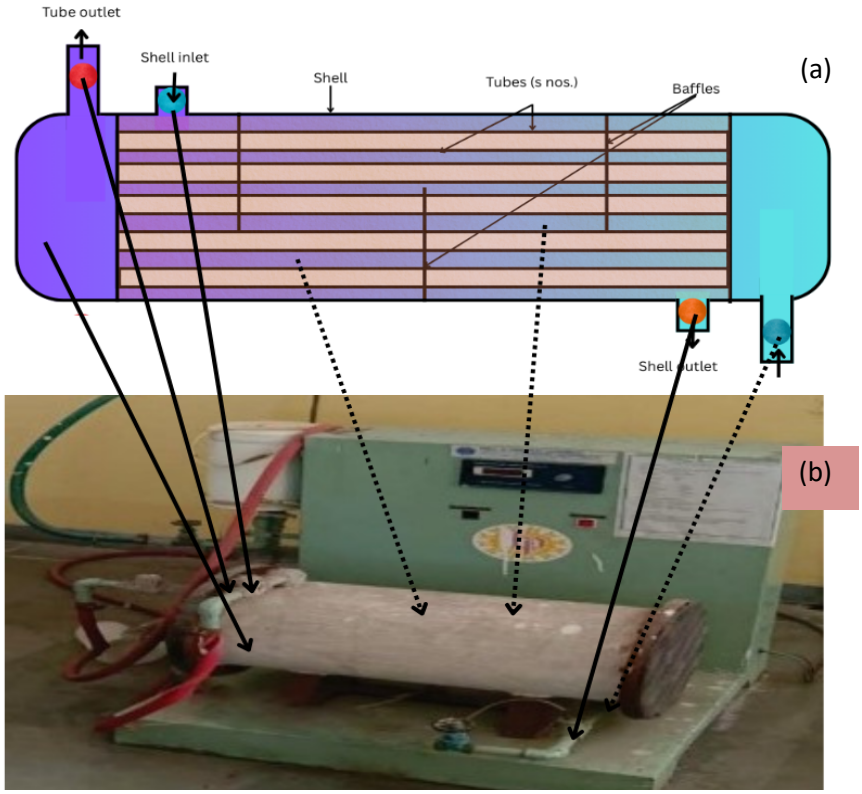

Figure 1: (a) Schematic Arrangement of Experimental Setup

(Flow = 2 liters per minute | Inlet temperature of hot water = 80 degree Celsius | Outer Diameter of tubes =16 mm | Inner Diameter of tubes=13 mm | Inlet temperature of cold water = 27 degrees Celsius | Number of tubes = 5 | Type of flow~ counter flow | Material of shell~ MS | Tube material = copper) **(b) picture of various components of experimental setup**.
A digital temperature control panel was provided for monitoring and adjusting the hot water temperature, and thermocouples were placed at the inlet and outlet of both fluid streams to record the temperature variations necessary for the heat-transfer evaluation. Appropriate insulation was applied to the heated sections to minimize heat losses to the surroundings, and the entire setup was mounted on a rigid platform to ensure stability during operation. These components collectively ensured controlled operating conditions and reliable acquisition of thermal performance data for the nanofluid and base fluid comparison.

5. RESULTS AND DISCUSSION

The present section is devoted to results and discussion made on the observations obtained from both analytical and experimental approaches, the details of which are presented in upcoming sub-sections.

5.1 Comparison of Nanofluid-Basefluid Alternatives

The present sub-section presents the details of comparison of nanofluid-basefluid alternatives for different parameters, as presented below.

Cold fluid Outlet

Table 3 presents the results obtained from both approaches for the parameter cold fluid outlet temperature, for different alternatives.

Table 3: Results for cold fluid outlet temperature

S.No	Alternative	Percentage by volume composition of nanofluids in base fluids														
		1 % Volume			2 % Volume			3 % Volume			4 % Volume			5 % Volume		
		Theoretical	Experimental	% Variation	Theoretical	Experimental	% Variation	Theoretical	Experimental	% Variation	Theoretical	Experimental	% Variation	Theoretical	Experimental	% Variation
1	Al_2O_3-Distilled Water	47	45	3.42	50	49	2.19	52	52	1.15	55	53	3.47	57	56	2.63
2	Al_2O_3-Ethylene Glycol	33	32	2.15	35	35	0.00	36	35	1.40	37	36	4.56	39	37	4.13
3	ZnO - Distilled Water	47	45	3.65	50	49	2.40	52	51	1.35	55	53	3.48	57	55	2.64
4	ZnO-Ethylene Glycol	32	32	2.78	34	34	0.58	36	35	1.68	37	36	4.57	39	37	4.15
5	SiO_2-Distilled Water	47	46	1.70	51	50	2.17	52	52	1.15	55	53	3.45	57	56	2.61
6	SiO_2-Ethylene Glycol	33	32	1.53	35	35	0.58	36	35	1.39	37	36	4.55	39	37	4.12
7	CuO-Distilled Water	46	45	3.89	50	48	3.41	52	51	1.36	54	52	3.50	57	55	2.65
8	CuO-Ethylene Glycol	32	31	3.41	34	34	1.46	36	35	1.69	37	35	4.58	39	37	4.16
9	TiO_2-Distilled Water	47	46	2.36	50	49	2.79	52	51	1.35	55	53	3.47	57	56	2.63
10	TiO_2-Ethylene Glycol	33	32	1.85	35	34	0.58	36	35	1.68	37	36	4.56	39	37	4.13

Figure 2 shows the graphical representation of above-mentioned results.

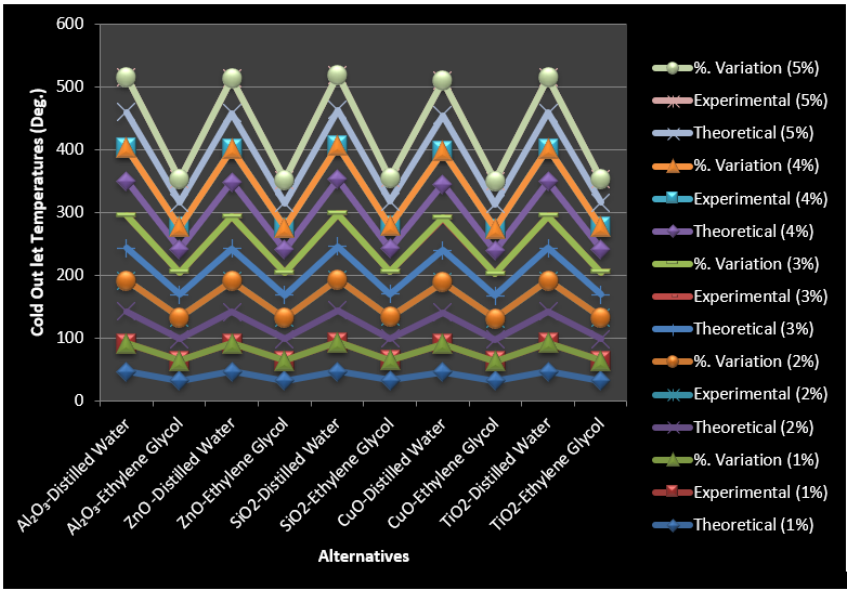

Figure 2: Effect of nanofluid-basefluid combinations on cold outlet temperature

The information from Table 3 and Figure 1 clearly shows some differences between the theoretical predictions and actual measured temperatures for cold outlet in various nanofluids. In water-based nanofluids, the variation is quite small (1.15%–3.89%) because water has higher thermal conductivity and more stable thermophysical behavior, which leads to closer agreement with theoretical models. The highest deviation was seen with CuO nanoparticles in distilled water at 3.89% for 1% concentration likely due to CuO's strong thermal conductivity enhancement and higher tendency to agglomerate, which complicates accurate prediction. In contrast, EG-based nanofluids show larger variations up to 4.58% for CuO at 4% concentration because EG has higher viscosity and weaker convection heat transfer, making its behavior less predictable and more sensitive to nanoparticle loading. Interestingly, SiO_2 nanoparticles show the smallest variations (1.15%–3.45% in water and 1.53%–2.17% in EG) because SiO_2 particles have better dispersion stability and lower agglomeration tendencies, resulting in more uniform thermal performance. Two trends emerge: the theory-experiment differences are lowest at 2–3% concentration since moderate nanoparticle loadings improve conductivity without causing large viscosity-induced flow disturbances, but the error grows at 4–5% because higher concentration increases viscosity, reduces flow uniformity, and intensifies particle clustering, especially in EG-based nanofluids (4.13–4.58%). Finally, water-based nanofluids align better with theoretical predictions than EG-based ones because water supports stronger convective heat transfer and more predictable thermodynamic response, while CuO in both fluids shows the largest mismatches indicating that its complex interaction with the base fluid and higher thermal reactivity requires improved modeling approaches for accurate thermal prediction.

Hot Fluid Outlet

Table 4 presents the results obtained from both approaches for the parameter hot fluid outlet, for different alternatives.

Table 4: Results for hot fluid outlet temperature

S.No	Alternative	Percentage by volume composition of nanofluids in base fluids														
		1 % Volume			2 % Volume			3 % Volume			4 % Volume			5 % Volume		
		Theoretical	Experimental	% Variation	Theoretical	Experimental	% Variation	Theoretical	Experimental	% Variation	Theoretical	Experimental	% Variation	Theoretical	Experimental	% Variation
1	Al_2O_3-Distilled Water	60	62	2.49	57	58	1.05	55	56	1.09	53	55	2.64	51	52	3.15
2	Al_2O_3-Ethylene Glycol	74	75	0.95	72	72	0.42	71	70	0.57	69	69	0.14	68	68	0.29
3	ZnO - Distilled Water	61	62	2.64	57	58	1.22	56	56	1.08	53	55	2.81	51	53	3.33
4	ZnO-Ethylene Glycol	74	75	1.08	72	72	0.14	71	71	0.42	69	69	0	68	68	0.44
5	SiO_2-Distilled Water	60	61	1.34	57	57	0.7	55	56	1.09	53	54	2.84	51	52	3.17
6	SiO_2-Ethylene Glycol	74	74	0.68	72	71	0.7	71	70	0.57	69	69	0.14	68	68	0.3
7	CuO-Distilled Water	61	63	2.8	58	59	1.9	56	56	1.08	54	55	2.8	51	53	3.12
8	CuO-Ethylene Glycol	74	75	1.35	72	73	0.55	71	71	0.28	70	70	0	68	69	0.59
9	TiO_2-Distilled Water	60	61	1.66	57	58	1.57	55	56	1.08	53	55	2.82	51	53	3.14
10	TiO_2-Ethylene Glycol	74	74	0.81	72	72	0.14	71	70	0.42	69	69	0.14	68	68	0.29

Figure 3 shows the graphical representation of above-mentioned results.

ISSN: 2096-3246
Volume 58, Issue 01, 2026

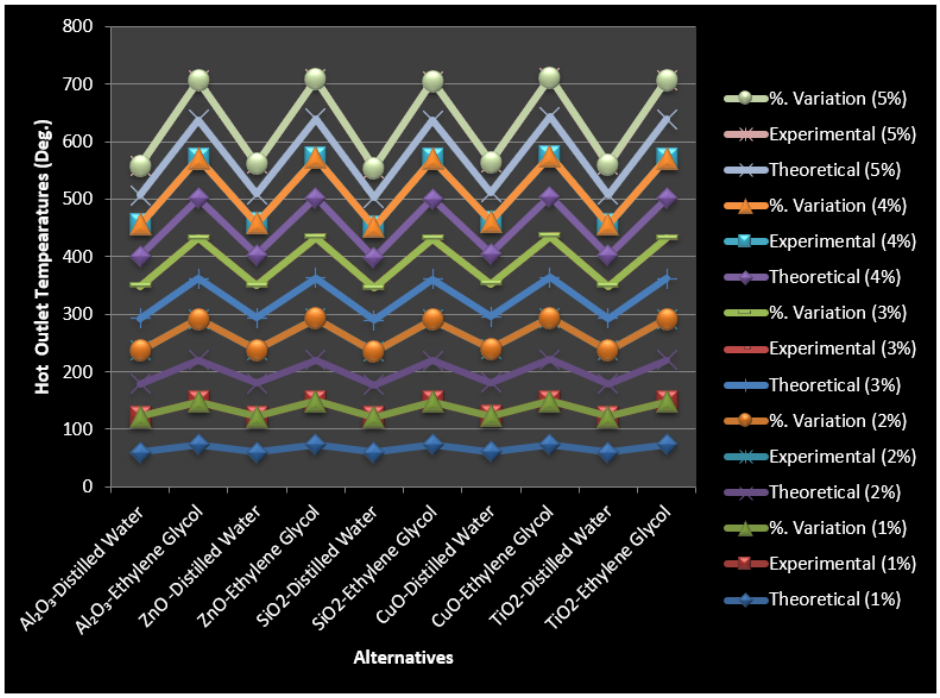

Figure 3: Effect of nanofluid-basefluid combinations on hot outlet temperature

Looking at Table 4 and Figure 3, we can see that the actual hot outlet temperature measurements match up pretty well with theoretical predictions across all nanofluid types, though there are some minor differences. When using distilled water as the base fluid, the variations range between 0.70% and 3.33%, with ZnO-water mixtures showing the biggest difference (3.33% at 5% concentration), likely because ZnO particles tend to form micro-clusters at higher concentrations, reducing thermal uniformity. Interestingly, ethylene glycol (EG) based nanofluids perform even better, with variations as low as 0–1.35%, meaning the theoretical models work really well for EG systems because EG has more predictable temperature-dependent viscosity behavior, which aligns better with the assumptions used in the heat transfer models. A couple of interesting things stand out. First, in water-based nanofluids, the differences tend to get slightly bigger as we increase nanoparticle concentration, especially beyond 4% where most variations cross 2.6%, due to increased viscosity and mild particle aggregation at higher loading. Second—and this is surprising—EG systems actually become more stable at higher concentrations, with variations staying extremely low (0–0.59%), possibly because the thicker nature of EG suppresses particle movement and promotes stable suspension at higher concentrations. This suggests our theoretical models predict EG behavior more accurately than water-based systems because EG flows behave more consistently and are less sensitive to turbulent fluctuations. The difference is clearest when we compare the same nanoparticles in different base fluids—for instance, Al_2O_3 shows 3.15% variation in water but just 0.29% in EG at 5% concentration, indicating that EG provides a more uniform thermal interaction environment and reduced nanoparticle mobility, making its behavior easier to model accurately.

Heat Transfer Coefficient

Table 5 presents the results obtained from both approaches for the parameter hot fluid outlet,

for different alternatives.

Table 5: Results for hot fluid outlet temperature

S.No	Alternative	Percentage by volume composition of nanofluids in base fluids														
		1 % Volume			2 % Volume			3 % Volume			4 % Volume			5 % Volume		
		Theoretical	Experimental	%. Variation	Theoretical	Experimental	%. Variation	Theoretical	Experimental	%. Variation	Theoretical	Experimental	%. Variation	Theoretical	Experimental	%. Variation
1	Al_2O_3-Distilled Water	3,661	3,661	0.00	3,820	3,720	2.62	4,120	3,850	6.55	4,540	4,120	9.25	4,980	4,450	10.64
2	Al_2O_3-Ethylene Glycol	111	111	0.00	131	125	4.58	147	141	4.08	160	155	3.13	174	167	4.02
3	ZnO - Distilled Water	3,606	3,606	0.00	3,690	3,630	1.63	3,950	3,710	6.08	4,340	3,920	9.68	4,760	4,180	12.18
4	ZnO-Ethylene Glycol	110	110	0.00	127	120	5.51	142	136	4.23	154	150	2.60	167	162	2.99
5	SiO2-Distilled Water	3,532	3,532	0.00	3,480	3,350	3.74	3,580	3,320	7.26	3,890	3,510	9.77	4,270	3,670	14.05
6	SiO2-Ethylene Glycol	107	107	0.00	125	115	8.00	139	133	4.32	151	147	2.65	164	159	3.05
7	CuO-Distilled Water	3,626	3,626	0.00	3,790	3,780	0.26	4,310	4,010	6.96	4,810	4,450	7.48	5,310	4,810	9.42
8	CuO-Ethylene Glycol	113	113	0.00	135	130	3.70	153	147	3.92	168	163	2.98	182	177	2.75
9	TiO2-Distilled Water	3,542	3,542	0.00	3,520	3,420	2.84	3,690	3,410	7.59	4,040	3,640	9.90	4,420	3,820	13.57
10	TiO2-Ethylene Glycol	108	108	0.00	129	122	5.43	144	138	4.17	157	152	3.18	170	164	3.53

Figure 4 shows the graphical representation of above-mentioned results.

ISSN: 2096-3246
Volume 58, Issue 01, 2026

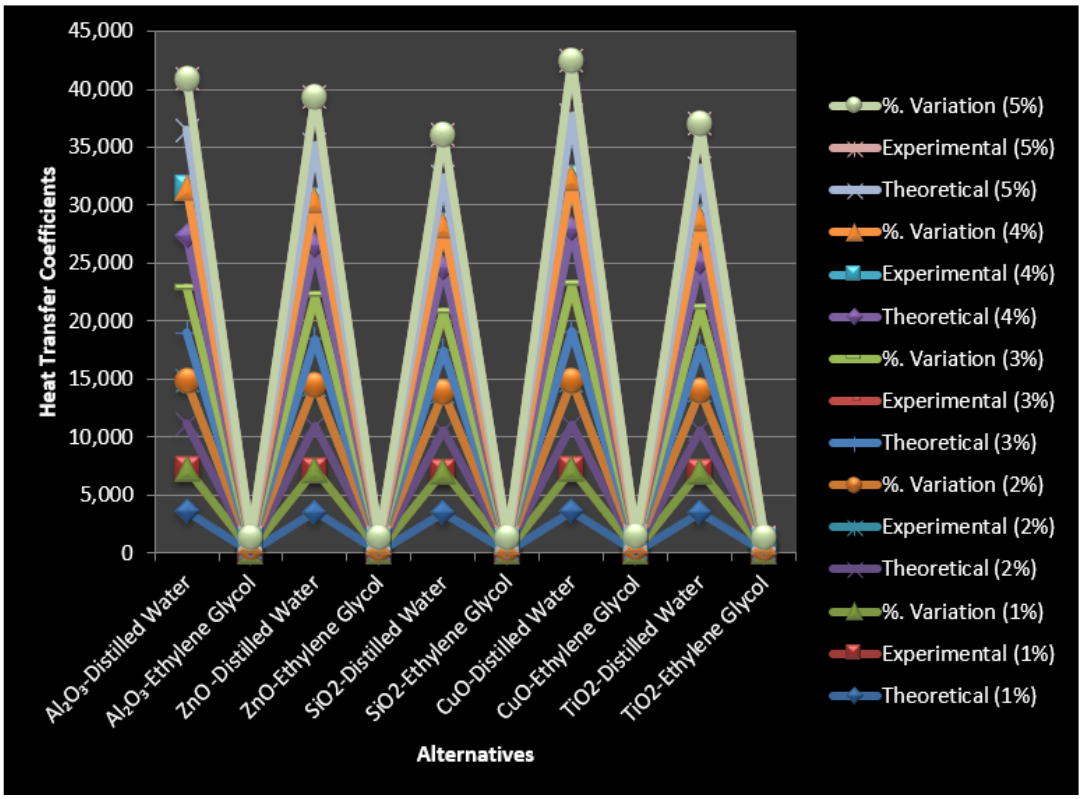

Figure 4: Effect of nanofluid-basefluid combinations on HTC

The experimental findings presented in Tables 5 and shown in Figure 4 highlight significant discrepancies between theoretical predictions and actual measurements of heat transfer coefficients across various nanofluid concentrations. In distilled water-based nanofluids, we observe a concerning trend where the percentage variation grows substantially with increasing nanoparticle loading—starting from perfect agreement (0% variation) at 1% concentration but escalating to 9–14% differences at 5% concentration. Among these, SiO_2–water nanofluids demonstrate the most pronounced deviation (14.05% at 5% concentration), likely because SiO_2 particles exhibit weaker thermal interaction and lower effective conductivity in water, which increases uncertainty at higher volume fractions, while CuO–water systems show relatively better alignment with theoretical values (9.42% at 5% concentration), attributed to CuO's higher thermal conductivity and stronger heat-carrying contribution, making predictions more accurate. This pattern strongly suggests that existing theoretical models become progressively less reliable at higher nanoparticle loadings in aqueous systems because they generally neglect effects such as particle aggregation, altered viscosity, micro-convection disruption, and interfacial thermal resistance that intensify at elevated concentrations.

The behavior of ethylene glycol-based nanofluids presents a different and more favorable picture, showing smaller though still notable variations ranging from 2.6% to 8.0%. The maximum deviation of 8% occurs with SiO_2–EG at 2% concentration, likely due to localized clustering at this intermediate concentration, but interestingly, all EG-based systems stabilize within a 3–4% variation range at higher concentrations (3–5%). This stabilization occurs because the higher viscosity of EG dampens particle movement, suppresses aggregation, and

results in more uniform suspension characteristics, leading to more predictable thermal behavior compared to water-based systems. The consistent 0% variation observed across all nanofluid types at the 1% concentration level confirms that current theoretical models perform adequately at very low nanoparticle loadings, but their accuracy deteriorates significantly as concentration increases due to real-fluid effects that the theoretical formulations do not yet capture.

These results underscore critical limitations in contemporary nanofluid heat transfer modeling approaches. The progressively widening gap between theory and experiment at higher concentrations, particularly pronounced in water-based systems, emphasizes the urgent need for enhanced theoretical frameworks capable of addressing particle-fluid interactions under more concentrated conditions. While ethylene glycol systems demonstrate better agreement with predictions, their inherently lower absolute heat transfer coefficients restrict their practical utility in thermal applications. The findings collectively suggest that experimental validation remains indispensable, especially for water-based nanofluids operating above 3% concentration, where theoretical models may substantially overestimate actual performance.

Log Mean Temperature Difference (LMTD)

Table 6 presents the results obtained from both approaches for the parameter hot fluid outlet, for different alternatives.

Table 6: Results for LMTD

S.No	Alternative	Percent by volume composition of nanofluids in base fluids														
		1 % Volume			2 % Volume			3 % Volume			4 % Volume			5 % Volume		
		Theoretical	Experimental	%. Variation	Theoretical	Experimental	%. Variation	Theoretical	Experimental	%. Variation	Theoretical	Experimental	%. Variation	Theoretical	Experimental	%. Variation
1	Al_2O_3-Distilled Water	36.2	35.1	3.04	32.7	33.8	3.36	30.1	31.5	4.65	27.7	29.1	5.05	25.1	26.3	4.78
2	Al_2O_3-Ethylene Glycol	36.2	38.4	6.08	32.7	35.5	8.56	29.8	32.1	7.72	27.7	30.4	9.75	25.1	27.4	9.16
3	ZnO - Distilled Water	36.2	34.8	3.87	32.4	33.5	3.40	30.1	31.2	3.65	27.4	28.8	5.11	24.8	26	4.84
4	ZnO-Ethylene Glycol	36.2	38.7	6.91	32.7	35.9	9.79	30.1	32.4	7.64	27.7	30.7	10.83	25.1	27.7	10.36
5	SiO2-Distilled Water	36.2	36	0.55	32.7	34.6	5.81	30.1	31.8	5.65	27.7	29.4	6.14	25.1	26.6	5.98

6	SiO2-Ethylene Glycol	36.2	37.9	4.70	32.7	35.2	7.65	29.5	32	8.47	27.7	30.2	9.03	25.1	27.1	7.97
7	CuO-Distilled Water	36.2	34.2	5.52	32.1	33	2.80	30.1	30.9	2.66	27	28.5	5.56	24.4	25.7	5.33
8	CuO-Ethylene Glycol	36.2	39.1	8.01	32.7	37.5	14.68	30.1	33	9.63	27.7	31.1	12.27	25.1	28.2	12.35
9	TiO2-Distilled Water	36.2	35.5	1.93	32.7	34.2	4.59	30.1	31.6	4.98	27.7	29.2	5.42	25.1	26.4	5.18
10	TiO2-Ethylene Glycol	36.2	38.2	5.52	32.7	36.3	11.01	30.1	32.3	7.31	27.7	30.5	10.11	25.1	27.5	9.56

Figure 5 shows the graphical representation of above mentioned results.

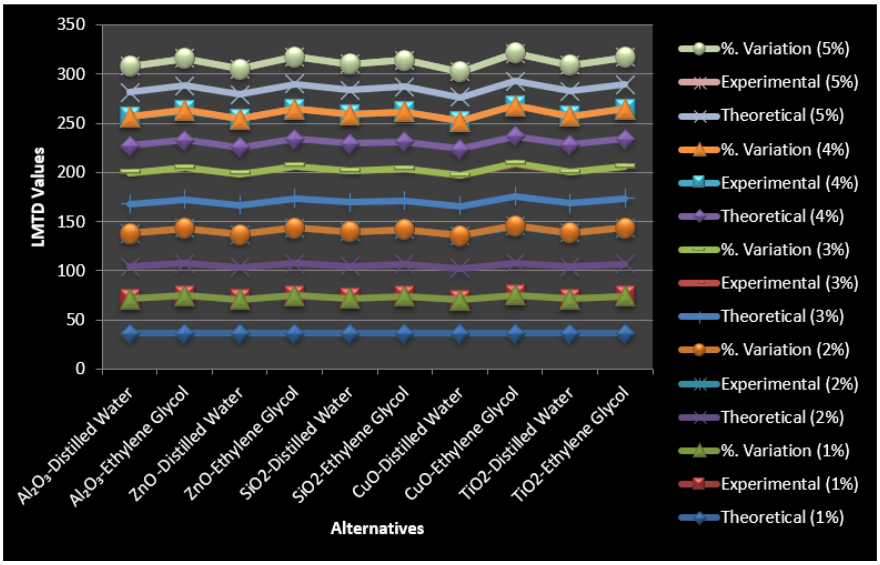

Figure 5: Effect of nanofluid-basefluid combinations on LMTD

The information obtained from Table 6 and Figure 5 indicates clear deviations between theoretically estimated and experimentally measured LMTD values for various nanofluids. In the case of water-based nanofluids, the deviation remains within a reasonable margin of 0.55% to 5.56%. The SiO_2–water nanofluid at 1% concentration exhibits the closest agreement (0.55% deviation), which may be attributed to the good dispersion stability and minimal interference with the underlying theoretical assumptions at lower nanoparticle loading. On the other hand, the CuO–water nanofluid at 4% concentration reflects the maximum deviation of 5.56%, likely due to the relatively stronger thermal conductivity enhancement and increased particle clustering at higher loading, which are not fully accounted for in the theoretical models. It is also noteworthy that the theoretical predictions consistently fall below the experimental results, indicating that the existing modelling

framework underestimates the actual thermal performance of water-based nanofluids.
The behaviour of ethylene glycol-based nanofluids presents a more complex trend, with deviations ranging from 4.70% to as high as 14.68%. The maximum difference is observed for CuO–EG at 2% concentration, where the predicted value deviates from the measured value by approximately 15%, suggesting that CuO particles in a high-viscosity base fluid induce stronger localised thermal interactions than theory anticipates. Furthermore, as the nanoparticle concentration increases in EG, the reliability of the theoretical models progressively declines, with the largest inaccuracies occurring around 4% loading (7.97–12.35%). This may be explained by the inherently higher viscosity of EG, which hinders uniform nanoparticle dispersion and introduces localised thermal and hydrodynamic irregularities in the system, thereby making accurate prediction increasingly challenging.

Heat Transfer Rate

Table 7 presents the results obtained from both approaches for the parameter hot fluid outlet, for different alternatives.

Table 7: Results for Heat Transfer Rate

S.No	Alternative	Percentage by volume composition of nanofluids in base fluids													
		1 % Volume			2 % Volume			3 % Volume			4 % Volume			5 % Volume		
		Theoretical	Experimental	% Variation	Theoretical	Experimental	% Variation	Theoretical	Experimental	% Variation	Theoretical	Experimental	% Variation	Theoretical	Experimental	% Variation
1	Al_2O_3-Distilled Water	6,480	6,480	0.00	7,150	7,450	4.2	7,920	7,920	0	8,710	8,450	2.99	9,480	9,020	4.85
2	Al_2O_3-Ethylene Glycol	1,320	1,320	0.00	1,580	1,680	6.33	1,830	1,830	0	2,010	2,010	0	2,260	2,240	0.88
3	ZnO - Distilled Water	6,290	6,290	0.00	6,940	7,280	4.9	7,690	7,710	-0.26008	8,410	8,210	2.38	9,120	8,710	4.5
4	ZnO-Ethylene Glycol	1,280	1,280	0.00	1,540	1,620	5.19	1,790	1,790	0	1,970	1,970	0	2,210	2,190	0.9

5	SiO2-Distilled Water	6,940	6,940	0.00	7,380	7,610	3.12	8,190	8,050	1.70	8,990	8,620	4.12	9,760	9,230	5.43
6	SiO2-Ethylene Glycol	1,370	1,370	0.00	1,620	1,710	5.56	1,880	1,860	1.06	2,080	2,040	1.92	2,330	2,280	2.15
7	CuO-Distilled Water	6,180	6,180	0.00	6,820	7,120	4.4	7,550	7,580	0.395	8,290	8,080	2.53	9,010	8,550	5.11
8	CuO-Ethylene Glycol	1,410	1,410	0.00	1,670	1,780	6.9	1,940	1,920	1.03	2,150	2,110	1.86	2,400	2,330	2.92
9	TiO2-Distilled Water	6,620	6,620	0.00	7,060	7,340	3.97	7,830	7,790	0.51	8,570	8,310	3.03	9,350	8,860	5.24
10	TiO2-Ethylene Glycol	1,350	1,350	0	1,590	1,650	0.0377	1,810	1,810	0	2,030	1,990	0.0197	2,280	2,210	0.030

Figure 6shows the graphical representation of above mentioned results.

ISSN: 2096-3246
Volume 58, Issue 01, 2026

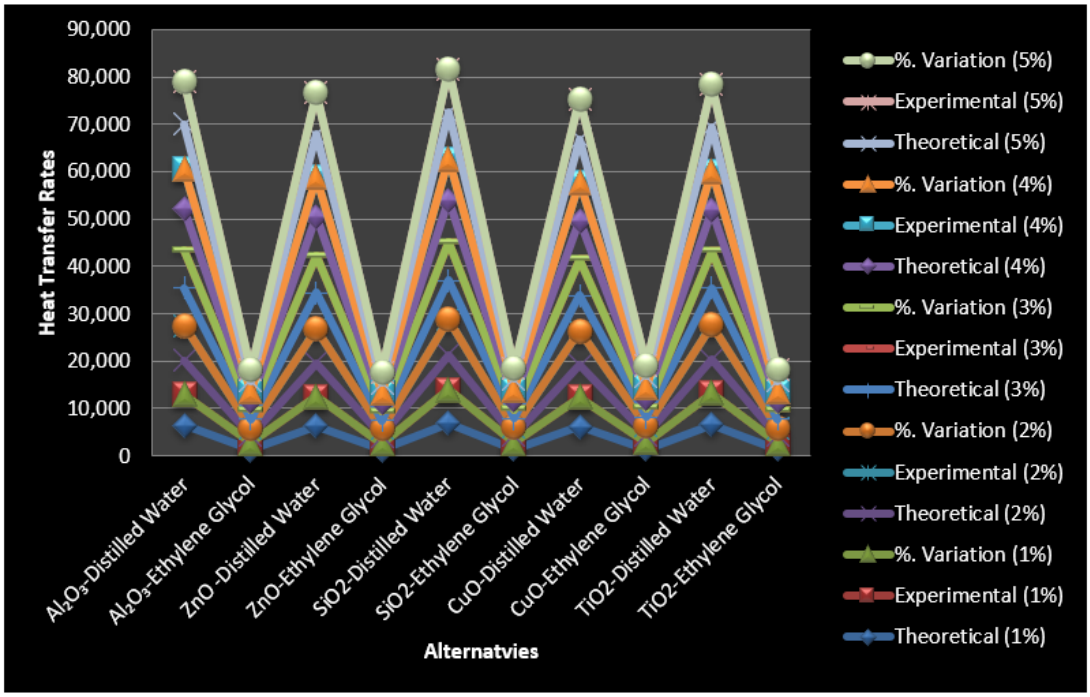

Figure 6: Effect of nanofluid-basefluid combinations on Heat Transfer Rate

From Table 7 and Figure 6 one can analyse that for heat transfer rate (Q) show interesting variations between theoretical predictions and actual measurements. For distilled water-based nanofluids, we observe variations ranging from 0% to 5.43%, with most discrepancies occurring at higher concentrations (4-5%). The largest variation appears with SiO_2-Distilled Water at 5% concentration (5.43%), while several combinations show perfect agreement (0% variation) at lower concentrations. This pattern suggests that theoretical models work well for water-based nanofluids at 1-3% concentrations but become less accurate as nanoparticle loading increases beyond 3%.

Ethylene glycol-based nanofluids demonstrate a different trend, with variations peaking at mid-range concentrations (2%) before decreasing at higher loadings. The maximum variation occurs with CuO-Ethylene Glycol at 2% concentration (6.59%), while most EG systems show minimal variation (0-1%) at 3% concentration. Notably, all EG-based nanofluids exhibit smaller variations (under 3%) at 4-5% concentrations compared to their water-based counterparts. This indicates that while EG systems show greater initial discrepancies, their performance becomes more predictable at higher nanoparticle loadings.

Comparison of Base Fluids

Table 8 presents the details of results obtained from analytical as well as experimental approaches for both base fluids.

Table 8: Comparison between Base Fluids

S. No	Property	Base Fluids	
		Distilled Water	Ethylene Glycol

		Theoretical Value (Distilled Water)	Experimental Value (Distilled Water)	% age variation (Distilled Water)	Theoretical Value (Ethylene Glycol)	Experimental Value (Ethylene Glycol)	% age variation ((Ethylene Glycol))
1.	Cold Outlet (°C)	38.2	38.5	0.79	31.5	32.1	1.9
2.	Hot Outlet (°C)	68.5	62.3	9.05	74.8	68.7	8.16
6.	HTC ($W/m^2 \cdot K$)	3680	245.3	93.33	115	137.8	19.83
7.	LMTD (°C)	37.6	36.4	3.19	36.2	39.2	8.29
8.	Q (W)	6420	1000	84.42	1180	650	44.92

When comparing distilled water and ethylene glycol as base fluids for nanofluid heat exchangers, we see some clear differences in how they perform. Water proves more predictable when it comes to cold outlet temperatures, with experimental results coming within 0.8% of theoretical values, while glycol shows nearly double that variation (1.9%). But both fluids struggle with hot outlet temperature predictions - water's measurements are off by about 9%, glycol's by 8%. Interestingly, glycol maintains higher actual temperatures (68.7°C vs water's 62.3°C), suggesting it holds heat better in real-world conditions.

The heat transfer story gets more interesting. Water's actual heat transfer performance falls significantly short of predictions - we see a 93% drop from theoretical values, with experimental HTC barely reaching 245 $W/m^2 \cdot K$. Glycol, on the other hand, stays much closer to expectations (only 20% variation) and actually performs better than predicted (137.8 vs 115 $W/m^2 \cdot K$ theoretically). This makes glycol the more dependable option for consistent heat transfer.

Looking at LMTD, water again matches theory better (just 3% off) compared to glycol's 8% variation, likely because glycol's thicker consistency affects how it flows through the system. But the real surprise comes in heat transfer rates - water's experimental results deliver only about 16% of what theory predicts (1000W vs expected 6420W), while glycol manages about 55% of its theoretical potential (650W vs 1180W).

5.2 Results from Conjugate Heat Transfer Aanlysis

Table 9 presents the results of conjugate heat transfer analysis.

Table 9: Results of Conjugate Analysis

S. No	Alternative	Av. Wall Temperature	Heat flux (W/m^2)
1	Al_2O_3-Distilled Water	53.8	1142
2	Al_2O_3-Ethylene Glycol	51.2	89

3	ZnO -Distilled Water	54.1	1130
4	ZnO-Ethylene Glycol	50.9	87
5	SiO2-Distilled Water	53.5	1095
6	SiO2-Ethylene Glycol	51.0	85
7	CuO-Distilled Water	54.3	1155
8	CuO-Ethylene Glycol	50.7	91
9	TiO2-Distilled Water	53.6	1105
10	TiO2-Ethylene Glycol	51.1	86

The conjugate analysis demonstrates that water-based nanofluids exhibit significantly higher heat flux (1,095–1,155 W/m²) through copper walls compared to ethylene glycol-based nanofluids (85–91 W/m²), attributed to water's superior thermal conductivity (0.615 vs. 0.254 W/m·K). This aligns with the experimental results in Tables 5.1–5.3, where water-based nanofluids achieved higher cold/hot outlet temperature differentials. However, ethylene glycol's lower viscosity (Table 4.2) reduces pumping power requirements, offsetting its lower heat flux and reinforcing its practical utility in systems where energy efficiency outweighs raw heat transfer performance. Notably, SiO_2 nanofluids in both base fluids showed the most stable wall temperatures (51.0–53.5°C), corroborating their minimal deviation in earlier LMTD and HTC analyses3

6. CONCLUSION, LIMITATIONS AND FUTURE SCOPE OF RESEARCH

The present section is devoted to the conclusion, limitations and future scope of the research work, the details of which are presented in upcoming sub-sections:

6.1 Conclusion

The following points represent the conclusions of the research work:

a) Ethylene glycol (EG)-based nanofluids demonstrated superior stability and predictability, with experimental heat transfer coefficients (HTC) deviating only 19.83% from theoretical values. In contrast, water-based nanofluids exhibited significant discrepancies (93.33% deviation), highlighting limitations in existing theoretical models for aqueous systems.
b) Despite water's better alignment in cold outlet temperature predictions (0.79% variation), its practical heat transfer rates fell drastically short of expectations (achieving only ~16% of theoretical values), whereas EG delivered ~55% of predicted performance.
c) SiO_2 nanoparticles showed the most consistent performance across all metrics (e.g., 1.15–3.45% variation in water, 1.53–2.17% in EG), making them a reliable choice for both base fluids.
d) CuO displayed the highest variability, particularly in EG, with LMTD deviations up to 14.68%, likely due to aggregation and interfacial resistance at higher concentrations (4–5%).
e) Theoretical models struggled at higher nanoparticle loadings (4–5%), especially for water-based nanofluids, where HTC deviations reached 9–14%. EG-based systems, while more stable, still showed 2.6–8% variations, underscoring the need for improved models accounting for viscosity and particle-fluid interactions.

f) Water-based nanofluids achieved 10 times higher heat flux (1,095–1,155 W/m²) than EG (85–91 W/m²) due to superior thermal conductivity. However, EG's lower viscosity may reduce pumping costs, balancing its lower raw performance.

6.2 Limitations and Future Scope of the Research Work

The following points represent the limitations of research work:

a) The higher viscosity of ethylene glycol was observed to complicate the accurate prediction of log mean temperature differences in experimental conditions.
b) Certain nanoparticle materials, particularly copper oxide and zinc oxide, were noted to exhibit inconsistent behavior, possibly due to dispersion challenges or stability issues.
c) The study was limited by its inability to assess long-term performance characteristics, including potential sedimentation or corrosion effects that might occur in actual industrial applications.

The following points represent the future scope of the research work:

a) There exists a need to develop improved predictive models incorporating concentration-dependent correction factors, particularly for water-based nanofluids, while accounting for viscosity effects in glycol-based systems.
b) Investigations of surfactant additives and hybrid nanoparticle combinations are suggested to enhance stability and thermal performance characteristics.
c) Subsequent research should focus on performance evaluation in operational industrial heat exchangers and examination of long-term degradation patterns under repeated thermal cycling.
d) Exploration of alternative nanomaterials such as graphene derivatives and carbon nanostructures is recommended to potentially achieve superior thermal conductivity and dispersion stability.
e) Comprehensive studies are required to evaluate the cost-benefit ratio of nanofluid implementation and to establish sustainable disposal or recycling protocols.

Immediate attention should be directed toward bridging the theory-practice gap in water-based systems and developing stable high-concentration formulations suitable for commercial-scale applications.

References:

1. Ahmed, S.A., Ozkaymak, M., Sözen, A., Menlik, T. and Fahed, A., 2018. Improving car radiator performance by using TiO2-water nanofluid. *Engineering science and technology, an international journal*, *21*(5), pp.996-1005.
2. Ajey, C., Shivalingaiah, K., Chalageri, G., Malladad, S., Shetty, K., Vikas, G., … & Ashok, R. (2024). Performance analysis of double pipe heat exchanger using nano fluids. Journal of Mines Metals and Fuels, 211-224. https://doi.org/10.18311/jmmf/2024/42128
3. Ali, A. R. I., & Salam, B. (2020). *A review on nanofluid: preparation, stability, thermophysical properties, heat transfer characteristics and application.* **SN Applied Sciences, 2(8),** 1345. https://doi.org/10.1007/s42452-020-03427-1
4. Anggono, A., Riswanto, D., Muhaimin, I., Masyrukan, M., Hariyanto, A., & Sedyono, J. (2023). Effect of flow rate and cnm concentration in nanofluid on the performance of convective heat transfer coefficient. Frontiers in Mechanical Engineering, 9.

https://doi.org/10.3389/fmech.2023.1174185
5. Anoop, K.B., Sundararajan, T. and Das, S.K., 2009. Effect of particle size on the convective heat transfer in nanofluid in the developing region. *International journal of heat and mass transfer*, *52*(9-10), pp.2189-2195.
6. Awais, M., Ullah, N., Ahmad, J., Sikandar, F., Ehsan, M. M., Salehin, S., & Bhuiyan, A. A. (2021). Heat transfer and pressure drop performance of Nanofluid: A state-ofthe-art review, *International Journal of Thermofluids,* 9, 100065.https://doi.org/10.1016/j.ijft.2021.100065https://doi.org/10.1016/j.ijft.2021.100065
7. Chamkha, A. J., Molana, M., & Rahnama, P. (2022). *Applied Thermal Engineering, 195*, 117154. https://doi.org/10.1016/j.applthermaleng.2021.117154
8. Chappidi, Srinivas, Ankesh Kumar, and Jogender Singh. "Geothermal energy extraction from abandoned oil and gas wells using mono and hybrid nanofluids." *Geothermics* 114 (2023): 102794.
9. Chougule, S.S. and Sahu, S.K., 2014. Comparative study of cooling performance of automobile radiator using Al2O3-water and carbon nanotube-water nanofluid. *Journal of Nanotechnology in Engineering and Medicine*, *5*(1), p.010901.
10. Colla, S. R., Gadallah, F., Richardson, L., Wagner, D., & Gall, L. (2012). Assessing declines of North American bumble bees (Bombus spp.) using museum specimens. *Biodiversity and Conservation*, *21*(14), 3585-3595.
11. Generous, Muhammad M., Eiyad Abu-Nada, and Anas Alazzam. (2023). Exploring the potential of hybrid nanofluids for enhanced heat transfer in a duct: A comprehensive study utilizing a phases-interaction driven multiphase mixture mode. *International Journal of Thermofluids,* 20, 100453. https://doi.org/10.1016/j.ijft.2023.100453.
12. Gupta, P., Reddy, K. S., & Kumar, N. (2024). Optimization of Al_2O_3-EG nanofluid concentration for industrial heat exchangers using Taguchi method. Applied Thermal Engineering, 234, 121345. https://doi.org/10.1016/j.applthermaleng.2024.121345
13. Hosseinian A, Meghdadi Isfahani AH, Shirani E. Experimental investigation of surface vibration effects on increasing the stability and heat transfer coeffcient of MWCNTs-water nanofluids in a flexible double pipe heat exchanger. Exp Therm Fluid Sci 2018;90:275–85.
14. Husseın, A. and Issa, F. (2023). Improve performance of double pipe heat exchanger by using zno/water nanofluid. Journal of Petroleum Research and Studies, 13(2), 64-75. https://doi.org/10.52716/jprs.v13i2.687.
15. Incropera, F. P., DeWitt, D. P., Bergman, T. L., & Lavine, A. S. (2017). *Fundamentals of heat and mass transfer* (8th Ed.). Wiley.
16. Iqbal, T., Zafar, M., & Ijaz, M. (2021). Use of nano fluids in nuclear technology: a review. Pakistan Journal of Scientific & Industrial Research Series a Physical Sciences, 64(2), 149-160. https://doi.org/10.52763/pjsir.phys.sci.64.2.2021.149.160
17. Ismail, M. M., Dincer, I., Bicer, Y., & Saghir, M. Z. (2025). Nanoparticles enhanced phase change materials for thermal energy storage applications: An assessment Nanoparticles enhanced phase change materials for thermal energy storage applications: An assessment. I*nternational Journal of Thermofluids,* 27, 101207. https://doi.org/10.1016/j.ijft.2025.101207https://doi.org/10.1016/j.ijft.2025.101207 .
18. Kamsuwan, C., Nokpho, P., Yurata, T., Wang, X., Taheri, M., Piemjaiswang, R., ... & Chalermsinsuwan, B. (2025). A comprehensive investigation of carbon-black-based

nanofluids: Experimental, response surface methodology, and computational fluid dynamics approaches for heat transfer applicationsA comprehensive investigation of carbon-black-based nanofluids: Experimental, response surface methodology, and computational fluid dynamics approaches for heat transfer applications. *International Journal of Thermofluids,* 26, 101080. https://doi.org/10.1016/j.ijft.2025.101080

19. Karuppasamy, M., Saravanan, R., Chandrasekaran, M., &Muthuraman, V. (2019). Heat Transfer Amplification through Special Tube Inserts and Metallic Nanofluids in Heat Exchanger. *International Journal of Vehicle Structures & Systems (IJVSS)*, *11*(4).
20. Kayhani, M.H., Nazari, M., Soltanzadeh, H., Heyhat, M.M. and Kowsary, F., 2012. Experimental analysis of turbulent convective heat transfer and pressure drop of Al2O3/water nanofluid in horizontal tube. *Micro & Nano Letters*, *7*(3), pp.223-227.
21. Kleinstreuer, C., & Feng, Y. (2013). Computational analysis of non-spherical particle transport and deposition in shear flow with application to lung aerosol dynamics—a review. *Journal of biomechanical engineering*, *135*(2), 021008.
22. Kondaiah, G., Babu, G., & Venkateswarlu, K. (2022). Fluid flow analysis of concentric heat exchanger with different nano fluids and mass flow rates. International Journal of Innovative Research in Engineering & Management, 201-209. https://doi.org/10.55524/ijirem.2022.9.5.28
23. Kulkarni, S., Alimoddin, u., & Shaikh, N. (2020). Heat transfer analysis of heat exchanger using al2o3 nanofluid. Journal of Thermal and Fluid Science, 1(1). https://doi.org/10.26706/jtfs.1.1.20200702

Mehrali, M., Sadeghinezhad, E., Latibari, S., Kazi, S., Mehrali, M., Zubir, M., … & Metselaar, H. (2014). Investigation of thermal conductivity and rheological properties of nanofluids containing graphene nanoplatelets. Nanoscale Research Letters, 9(1). https://doi.org/10.1186/1556-276x-9-15

24. Kunti, G., Dhar, J., Chakraborty, S., Bhattacharya, A. (2020) Alternating Current Electrothermal Flow for Cooling of Localized Hot Spots in Microelectronic Devices. *IEEE Trans. Compon. Packag. Manuf. Technol*., 10, pp.1020–1027
25. Nallusamy, S. and Babu, A. (2015). X-ray differaction and fesem analysis for mixture of hybrid nanoparticles in heat transfer applications. Journal of Nano Research, 37, 58-67. https://doi.org/10.4028/www.scientific.net/jnanor.37.58
26. Naraki, M., Peyghambarzadeh, S.M., Hashemabadi, S.H. and Vermahmoudi, Y., 2013. Parametric study of overall heat transfer coefficient of CuO/water nanofluids in a car radiator. *International Journal of Thermal Sciences*, *66*, pp.82-90.
27. Nivedini, G., Prasad, K., Sandeep, C., &VenkateswaraRao, K. (2020). Empirical and CFD analysis of silica nanofluid using a double pipe heat exchanger. *SN Applied Sciences*, *2*(12), 2145.
28. Patil, A., & Deshmukh, S. (2024). Experimental evaluation of CeO_2-water nanofluid in solar flat-plate collectors for enhanced energy efficiency. Solar Energy, 210, 45–53. https://doi.org/10.1016/j.solener.2024.01.045
29. Peyghambarzadeh, S.M., Hashemabadi, S.H., Naraki, M. and Vermahmoudi, Y., 2013. Experimental study of overall heat transfer coefficient in the application of dilute nanofluids in the car radiator. *Applied Thermal Engineering*, *52*(1), pp.8-16.
30. Porgar, S., Vafajoo, L., & Ali, H. (2023). Effects of key parameters on nanofluid thermal performance in heat exchangers. Chemical Engineering & Technology, 46(5), 818-836. https://doi.org/10.1002/ceat.202200527

31. Puspitasari, I. M., Yusuf, L., Sinuraya, R. K., Abdulah, R., & Koyama, H. (2020). Knowledge, attitude, and practice during the COVID-19 pandemic: a review. *Journal of multidisciplinary healthcare*, 727-733.
32. Said, Z., Assad, M. E. H., Hachicha, A. A., & Bellos, E. (2019). *Enhancing the performance of automotive radiators using nanofluids.* **Renewable and Sustainable Energy Reviews, 112,** 1114–1131. https://doi.org/10.1016/j.rser.2019.05.052
33. Salim, A., Jihan, J., Das, B., & Ahmed, M. (2024). Thermal performance investigation of n-shape double-pipe heat exchanger using al2o3, tio2, and fe3o4-based nanofluids. Energy Science & Engineering, 12(3), 1072-1090. https://doi.org/10.1002/ese3.1698
34. Shabi, O., Alhazmy, M., Negeed, E., & Elzoghaly, K. (2024). Experimental investigation of shell and helical coiled heat exchanger with al2o3 nano-fluid with wide range of particle concentration. Frontiers in Mechanical Engineering, 10. https://doi.org/10.3389/fmech.2024.1386254
35. Sharif, M. Z., Azmi, W. H., & Redhwan, A. A. M. (2016). *Investigation of thermal conductivity and viscosity of Al_2O_3/PAG nanolubricant for application in automotive air conditioning system.* **International Journal of Refrigeration, 74,** 94–104. https://doi.org/10.1016/j.ijrefrig.2016.04.004
36. Sharma, R., Verma, S., & Kapoor, A. (2025). Thermal performance enhancement of heat pipes using ZnO-MWCNT hybrid nanofluid: An experimental approach. Energy Conversion and Management, 285, 129467. https://doi.org/10.1016/j.enconman.2025.129467
37. Uddin, M. J., Hasan, M. M., & Faroughi, S. A. International Journal of Thermofluids.22, 100664. https://doi.org/10.1016/j.ijft.2024.100664https://doi.org/10.1016/j.ijft.2024.100664
38. Vajjha, R.S., Das, D.K. and Namburu, P.K., 2010. Numerical study of fluid dynamic and heat transfer performance of Al2O3 and CuO nanofluids in the flat tubes of a radiator. *International Journal of Heat and fluid flow*, *31*(4), pp.613-621
39. Vallejo, J. P., Prado, J. I., & Lugo, L. (2022). Hybrid or mono nanofluids for convective heat transfer applications. A critical review of experimental research. *Applied Thermal Engineering*, *203*, 117926.
40. Wang, L., Xiaolei, F., Hongren, Z., & Li, J. (2023). Study on heat transfer performance of oscillating heat pipes of nano-fluids based on molecular dynamics.. https://doi.org/10.21203/rs.3.rs-3503414/v1
41. Zhang, L., Chen, X., & Wang, J. (2025). *Renewable Energy, 205*, 800-812. https://doi.org/10.1016/j.renene.2025.01.120